

## T1 Carrier Characterization—Field-Measurement Results

By T. C. KAUP, D. G. LEEPER, A. K. REILLY, and  
P. E. SCHEFFLER

(Manuscript received February 8, 1980)

*We undertook a field-measurement program for T1 carrier to gain an understanding of crosstalk performance in the outside plant and office environments. This would help us to use the existing plant more efficiently and to predict the performance of future systems. Repeater-section lines were measured in the trunk plant of three Bell System operating companies during 1977 and 1978. Results given here include the distributions of repeater section crosstalk margin, noise, and various system and cable properties. We describe a T1 crosstalk engineering model which explains the significant contributions to section margin. The measurements and analysis show that repeater apparatus-case crosstalk dominates intermediate repeater-section performance, while the performance of sections adjacent to central offices (end sections) is limited by cable crosstalk with evidence of impulse noise present on some lines. Maximum use of cable and equipment for T1 and future digital transmission systems has been made much easier with the knowledge gained from these field measurements. For instance, the results of this program have already been used to redefine engineering rules for bidirectional cable operation, allowing more wire pairs in the cable to be used for T1 operation.*

### I. INTRODUCTION

The T1 repeatered line transmits a  $1.544 \times 10^6$  b/s bipolar signal on paired cable.<sup>1</sup> Since its introduction in 1962, its largest application has been as the transmission medium between D-channel banks that digitally encode and time-division-multiplex voice-frequency signals. A D/T1 system consists of two D-bank terminals and the transmission path of tandem T1 span lines interconnected at central offices along

the route between these terminals. Each span line is a series connection of T1 repeater sections between two central offices. Those sections adjacent to the offices are termed end sections; all others are referred to as intermediate sections.

The T1 error-rate objective specifies that at least 95 percent of 50-section systems shall have average transmission error rates less than  $10^{-6}$  errors per bit.<sup>2</sup> Since the digital signal is regenerated at each repeater location, the error performance of a T1 system is approximately equal to the accumulated performances of the individual repeater sections. Therefore, an understanding of T1 carrier repeater section performance and the elements that control that performance is needed to establish a model for system behavior.

Measurements were conducted in the trunk plants of three Bell System OTCS during 1977 and 1978 using the automated equipment described in Ref. 3. In all, approximately 2000 repeater section lines were examined in 30 different repeater sections.

Most of the measurements were performed on nearly full-length repeater sections (measured section lengths were about 6,100 feet for intermediate sections and about 4,000 feet for end sections), on 22-gauge pulp-paired cable, terminated with apparatus cases, each of which holds 25 discrete-component T1 repeaters. Other situations examined included sections terminated with repeater cases that hold 25 smaller-size integrated-circuit versions of the T1 repeater. These two measurement situations are identified in this paper as 466/201 and 475/208, respectively.

The primary measure of performance was *repeater section margin*, which is defined as the additional noise at the regenerator input that can be tolerated before a  $10^{-6}$  error rate is observed.

A margin model is shown here and the margin components identified from observations of various noise and section characteristics (e.g., noise spectrum and amplitude statistics, and cable-pair insertion loss). The individual measured quantities and the measurement techniques used are outlined in Ref. 3.

Section I of this paper briefly describes the measurement program. Section II gives the results of measurements of the primary performance parameter-repeater section margin. Section III outlines observed characteristics of crosstalk and office noise and the contribution of different types of crosstalk noise to repeater-section margin. Section IV describes a model for section margin and gives the measured characteristics of each element identified in this model. Section V characterizes plant parameters, such as cable insertion loss and examines the performance of repeater sections other than those having pulp cable with 466 apparatus cases and 201 repeaters; Section VI summarizes the key results of the measurement program.

## II. T1 REPEATER-SECTION MARGINS

Repeater-section margin, which is the incremental noise a section can tolerate before producing a  $10^{-6}$  error rate, was measured directly for intermediate repeater sections by attenuating the signal at the beginning of the section and amplifying the signal and noise by the same amount at the end of the section (just before the repeater input), as shown in Fig. 1. The amplification required to produce a  $10^{-6}$  error rate was recorded as the margin.

A modified procedure was used to measure end section margins, mainly due to the inconvenience of transporting the rather elaborate van-based measurement system into and out of central offices. In the absence of a T1 signal, the noise at the input of a T1 office repeater was amplified until errors (pulses) at a  $10^{-6}$  error rate were observed at the repeater output. The repeater, whose input section was set to equalize for the proper end-section cable loss, was clocked externally at a  $1.544 \times 10^6$  rate to simulate the clock that would normally be derived from a T1 signal. Thus, the margin for an "all zeroes" pulse sequence was obtained.

### 2.1 Intermediate section margins

Figure 2 displays the measured margin distribution obtained for intermediate sections for the standard 466/201 22-gauge pulp case. The margins were measured using the original service repeaters plugged into the apparatus cases. (Note: a second set of margins was measured using a particular Bell Laboratories test repeater. The difference in margins measured for test and service repeaters is discussed in Section 4.8.)

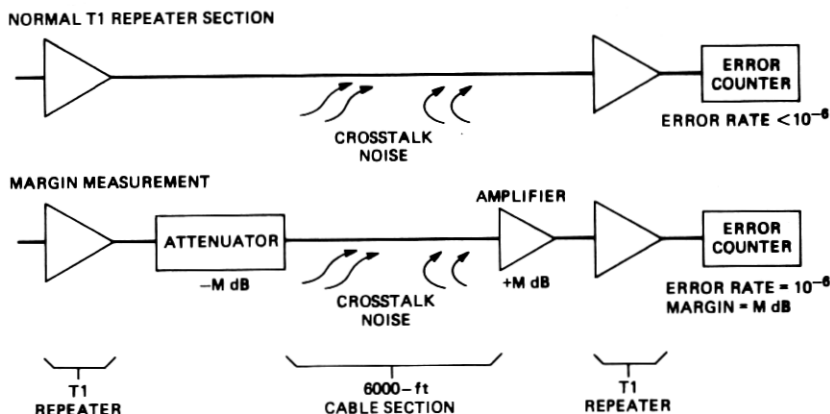


Fig. 1—Margin measurement by noise enhancement.

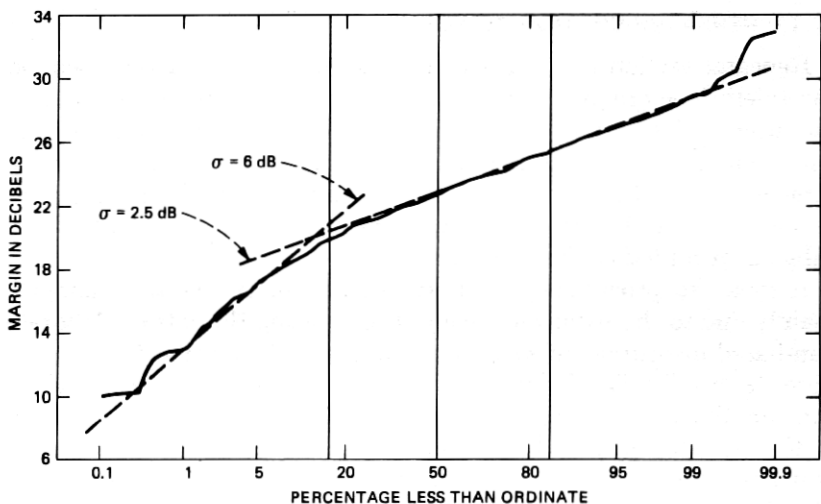


Fig. 2—Service margins (1977-78) for the 466/201 situation. Number of points = 915; average = 22.6; standard deviation = 3.03.

Each point on the curve shows the percent of repeater sections that have the indicated margin or less. The horizontal axis is a probability scale so that Gaussian distributions should appear as straight lines on the plot. The average section margin was 22.6 dB, for sections whose average cable insertion loss was 30.7 dB at 772 kHz (772 kHz is the half-baud for T1 transmission, which is near the major peak in the transmitted energy spectrum).

The minimum margin observed was 10 dB, a value for which essentially no errors due to intersystem crosstalk should be observed under normal conditions, even on lines comprising 50 such sections in tandem. However, the current measurements do not rule out widely separated impulses or noise bursts as a cause of errors, since the margin measurements were made for a period of only about 30 seconds on each repeater-section line.

The 0.1 percent point of the distribution may be estimated by drawing a straight line through the lower end of the curve as shown. This point on the distribution must have at least 3 dB of margin according to the repeater-section objective (Section IV). The estimated value is about 8.5 dB, which is 5.5 dB better than the objective.

To account for the *longest possible* repeater sections, the margins can be corrected to values expected for a section loss of 34 dB, the maximum loss allowed by engineering rules. Since the average loss for the margin measurements was 30.7 dB, the 0.1 percent margin is expected to be about 4.9 dB for systems composed of maximum length



sections.\* This is still 1.9 dB above the objective and represents a conservative estimate of actual system performance in the field, since most sections are less than full length.

The measured margin distribution may be divided into two regions, as is shown by the two straight lines drawn through the measured points. These regions correspond to different types of intersystem crosstalk as discussed in Section III. It should be noted that the low (worst margin) end of the distribution has poorer margins than would be expected, assuming a Gaussian distribution with mean and standard deviations equal to those values determined for the overall set of measurements.

In summary, intermediate repeater-section margins measured in the field easily meet section objectives. Therefore, intersystem crosstalk on intermediate sections is not expected to be a major source of errors on T1 lines.

## **2.2 End-section margins**

The amount of data collected for end sections (about 300 lines measured) in the field measurement program are much less than that collected for intermediate sections. Also, considering the wide variety of office environments possible, the end-section data are not likely to represent all T1 layouts that exist in the field today. Therefore, these data should be treated as a possibly biased sample of end-section performance.

End-section margins were measured in two OTCs on sections using 22-gauge pulp cable with 772-kHz cable losses ranging from 11.4 dB to 21.4 dB (section lengths from 2.2 to 4.1 kft). As shown in Fig. 3, the mean margin determined from the office-noise-amplification technique is 25.0 dB for all lines measured, with a standard deviation of 1.9 dB. The 0.1-percent point trend of the distribution is about 18 dB, if the one poor margin point at 14 dB is ignored.

All of the margins, however, should be adjusted downward to take into account intersymbol interference in normal repeater operation. (Remember that the end-section measurements were made in the absence of a T1 signal on the line.) This adjustment, if the office repeater degradation is the same as that found for the intermediate-section test repeater (see Section 4.7) would be about 4.3 dB. If the margins are adjusted by this amount, the average margin would be 20.7 dB, the minimum margin would be 9.7 dB, and the estimated 0.1 percent point (trend of the distribution) would be about 13.7 dB.

---

\* The correction of 3.6 dB in margin for a cable loss change of 3.3 dB assumes a proportionality factor of 1.09 between margin and cable loss. See discussion of noise power,  $I$ , in Section 4.5.1.

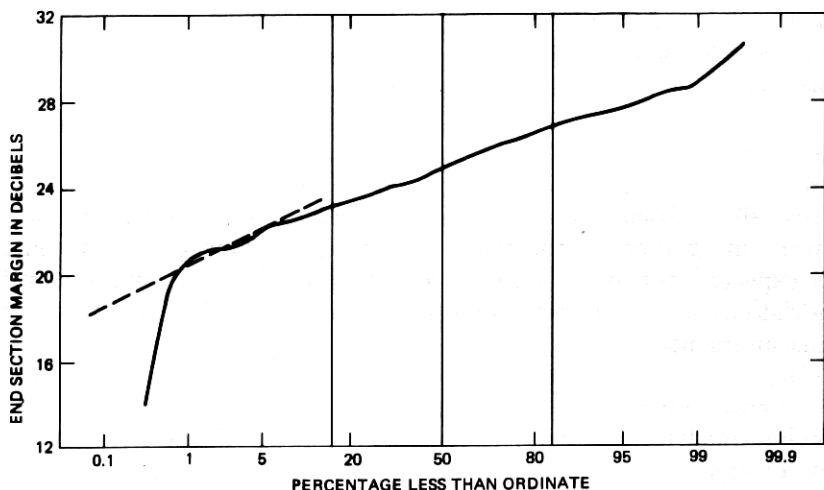


Fig. 3—End-section margins for the 466/201 situation. Number of points = 303; average = 25.0; standard deviation = 1.88.

The adjusted mean and minimum end-section margins are similar to the values found for intermediate-section measurements. However, the estimated 0.1-percent point of the end-section margin distribution is much higher than that for intermediate sections. Also, the standard deviation is smaller than for intermediate section measurements, despite the wider range of cable lengths. A possible explanation of these differences in terms of different types of crosstalk noise present is given in the next section.

Whether these data are truly representative of all end sections remains an open question. One conclusion from the above discussion is that the average performance of (these) end sections and intermediate sections are roughly the same; both layouts appear to have some reserve crosstalk margin that can possibly be exploited to pack more transmission channels into the same physical cable medium or, alternatively, to raise performance requirements.

### III. SOURCES OF NOISE FOR T1 CARRIER

In the original design analysis for T1 carrier,<sup>2</sup> allowances were made for noise due to near-end crosstalk (NEXT) and far-end crosstalk (FEXT) on intermediate repeater sections and for impulse noise due to office switching transients on end sections. Results from the field-measurement program reported here indicate that the dominant noise source for intermediate-repeater sections is crosstalk noise generated in the repeater apparatus case and stub cable (designated ACXT), rather than

NEXT or FEXT generated in the main cable. Also, the character of the noise for most of the end sections measured does not appear to be strongly impulsive, at least for measurement periods of one minute or less.

### 3.1 Intermediate repeater sections

Figure 4 illustrates the types of noise-coupling paths found in intermediate-repeater sections of a T-carrier span. Intersystem crosstalk (noise due to other T1 systems in the same cable) is dominant in intermediate sections; other sources of noise, such as thermal, may be neglected. Intersystem crosstalk of three types are shown:

(i) Cable near-end crosstalk (NEXT) caused by coupling between wire pairs in the main cable where the output (high level) pulse stream of a T1 repeater interferes with the input (low level) of the same or a nearby repeater.

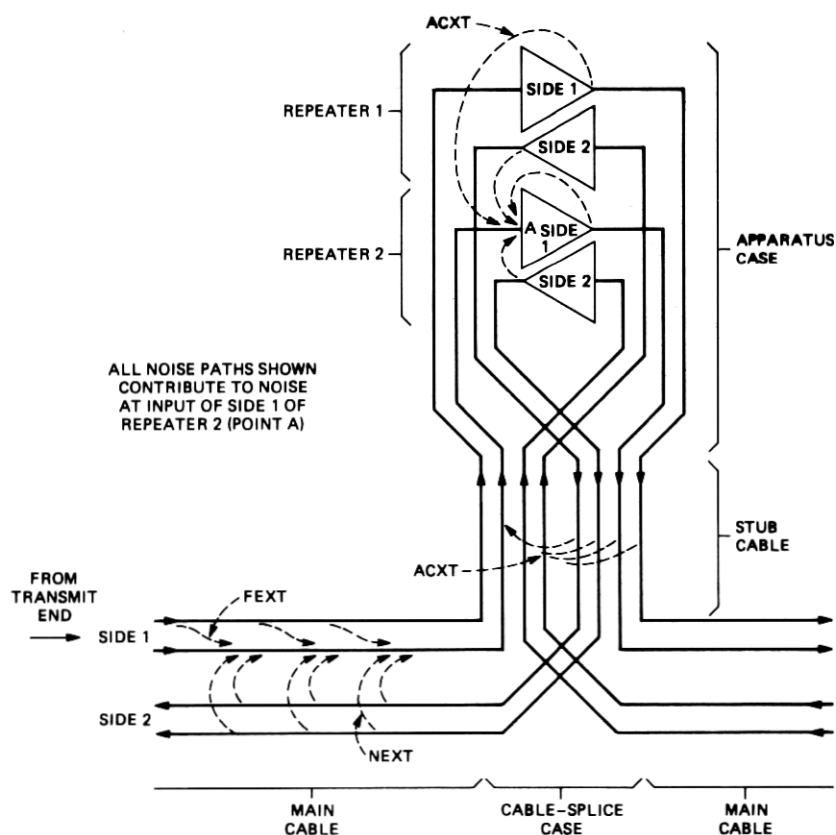


Fig. 4—Noise-coupling paths for intermediate-repeater sections. All noise paths shown contribute to noise at input of side 1 of repeater 2 (point A).

(ii) Cable far-end crosstalk (FEXT) caused by coupling between wire pairs in the main cable whose signals are propagating in the same direction and at the same level. Occasionally, T1 signals of different levels appear at the same point in the cable because two or more different routes merge at a point between repeaters. These are called incidental junctions. The increased FEXT noise resulting from this situation is not treated here.

(iii) Apparatus-case crosstalk (ACXT) caused by coupling in the wiring inside the apparatus case or in the case stub cable.

In standard T1 engineering layouts, main cable NEXT is negligible compared to ACXT and FEXT because opposite directions of transmission are segregated into binder groups on opposite sides of the cable as illustrated in Fig. 5. However, NEXT can be significant in some less commonly used configurations such as those described in Section 5.3.2. Assuming main-cable NEXT to be negligible for the standard configurations measured, the noise appearing at the repeater input was due to T1 sources with individual ones densities coupling through ACXT and

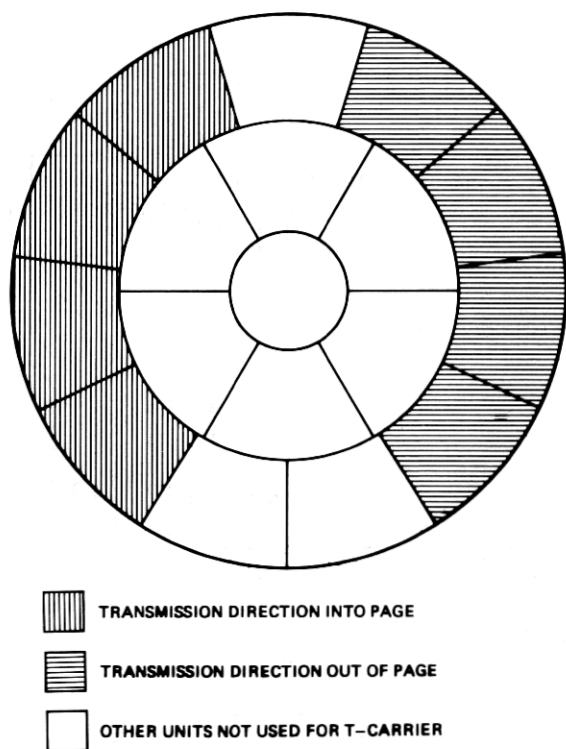


Fig. 5—Cable cross section showing use of cable units in a 900-pair, 22-gauge pulp cable with 200 active T1 systems.

FEXT paths of various losses. In the field measurement program, a simple means was found to separate the noise into ACXT and FEXT components and to determine an "effective" ones density for the disturbers.

### 3.1.1 Ones density ( $p$ ) and fraction ACXT ( $\alpha$ )

Based on measurements of the crosstalk noise-power density at the repeater input (before equalization), expected values for two parameters,  $p$  and  $\alpha$ , have been calculated from a fit of the data to eq. (15) of Appendix B where:

(i)  $p$  is the effective ones density of all of the disturbers defined as that single ones density that best fits the shape of observed noise spectrum.

(ii)  $\alpha$  is the fraction of the crosstalk noise density at 772 kHz at the repeater input that is attributable to ACXT.

The effective ones density of the disturbers proved to be a useful concept, even though it was known that all disturbers did not have the same ones density. Besides providing an indication of the average ones density (weighted by crosstalk coupling) in the T1 environment of the line being measured, it enabled a cleaner separation of the components of the noise spectrum, caused by ACXT and FEXT (i.e., the determination of  $\alpha$ ), than would otherwise be possible.

Distribution plots of  $p$  and  $\alpha$  are given in Figs. 6 and 7. Ones density,  $p$ , ranges from 0.5 to 0.95 with an average of 0.69. This is consistent with a combination of ones densities from the older D1 banks ( $<0.5$ )

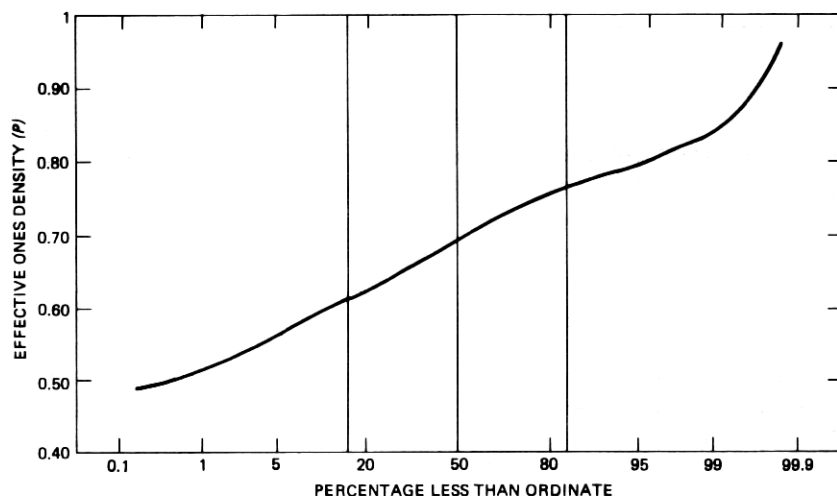


Fig. 6—Effective ones density,  $p$ , for the 466/201 situation. Number of points = 596; average = 0.69; standard deviation = 0.07.

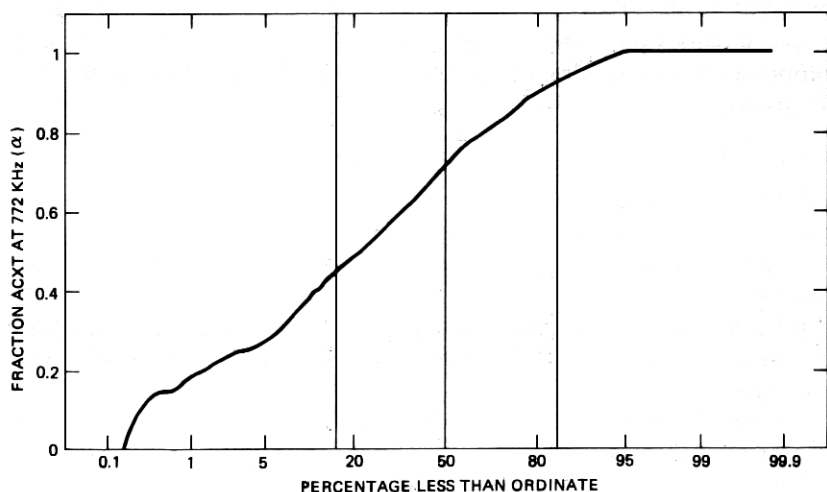


Fig. 7—Fraction ACXT at 772 kHz,  $\alpha$ , for the 466/201 situation. Number of points = 596; average = 0.69; standard deviation = 0.22.

and from the newer D1D or D3 banks ( $>0.8$ ). (In a few cases, it was known which bank predominated, and in these situations, the fitted value of  $p$  was seen to track the bank type.)

From Fig. 7,  $\alpha$  is seen to range from 0 to 1 with a mean value of 0.69. The fraction represented by  $\alpha$  is larger than 0.5 on 80 percent of the lines measured, indicating that ACXT tends to dominate over FEXT, at least at 772 kHz. Furthermore, in at least 5 percent of the measured lines, there is no observable FEXT at all ( $\alpha = 1$ ).

### 3.1.2 Predicted intermediate section margins

In Fig. 8, predicted margin distributions due to ACXT, FEXT, and NEXT, and their composite, are compared to measured repeater margins for the standard layout of 22-gauge pulp multipair unit cable and 466-type apparatus cases.

The ACXT and FEXT curves are based on calculated distributions of ACXT and FEXT noise powers for those T1 systems measured in the field. (See Section 4.4.) The NEXT distribution is based on published NEXT pair-to-pair statistics for remote- and alternate-unit coupling in a 900-pair, 22-gauge pulp cable, with 200 active T1 systems. The numerical details of the crosstalk and margin calculations appear in Appendix A.

The predicted margin distributions were calculated using the margin equation, (see Section 4.2), with the assumption that crosstalk noise was the only variable. Other parameters, such as the cable section loss, ones density of signals on the crosstalk disturbers, repeater degrada-

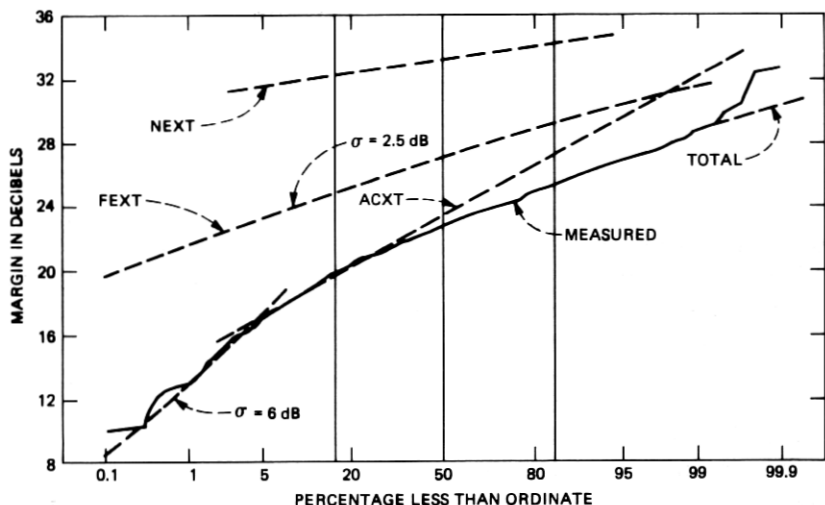


Fig. 8—Predicted service margins due to NEXT, FEXT, and ACXT. Number of points = 915; average = 22.6; standard deviation = 3.03.

tion, and peak factor of the noise, were held to the mean values observed over the course of the field measurements. (See discussion of these parameters in Section IV.)

From Fig. 8, it can be seen that the total derived margin distribution is dominated by apparatus-case crosstalk at the low margin end, which is the significant region for T1 engineering purposes. (The margin at the 0.1-percent point is the engineering parameter used to account for the longest metropolitan T1 systems, which consist of 50 repeater sections in tandem.) It is only at higher margins that FEXT makes a significant contribution to the total margin. Near-end crosstalk has a negligible effect on the total margin for all lines.

Since, for engineering purposes, it is only necessary to know the behavior of the distribution at the low-margin end, a model that only considers the contribution of ACXT is sufficient for predicting T1 performance. New system layouts, however, will use apparatus cases with reduced internal crosstalk coupling so that cable FEXT may become the limiting factor on performance for these systems. Also, any layout that allows opposite directions of transmission to be routed through adjacent binder groups or closer must take into account cable NEXT. (See Section 5.3.2.)

The close agreement of the predicted margin curves with measured data provides confidence that the major noise sources and coupling mechanisms that dominate margin performance of intermediate repeater sections are understood.

### 3.2 End-section noise environment

The noise sources and coupling paths for end sections vary more than those for intermediate sections, because of the multiplicity of cabling and equipment layouts, as well as switching type and activity occurring at offices at which through or terminating T-carrier systems appear. Figure 9 is a sketch of possible coupling paths for noise that eventually appears at the decision point of a T1 office repeater, but such noise paths are not completely known or characterized.

The end-section margin distribution (Fig. 3) has a standard deviation (1.9 dB) that is consistent with the predicted FEXT margin distribution (Fig. 8), but the average margin for end sections is worse than that predicted for intersystem FEXT alone. Other noise sources, perhaps office switching or traffic noise coupling through NEXT paths in the end-section cable, might be responsible for the difference.

Since we know that the office noise environment tends to be impulsive in nature because of switching activity, an effort was made to further characterize end-section noise observed in T1 office repeaters as either impulsive, Gaussian, or truncated by observing some characteristics of the noise-amplitude distribution. Figure 10 will help to illustrate the relationship between two parameters measured on each line.

The first parameter, the noise peak factor, is defined as the ratio (expressed in dB) of the repeater-error threshold voltage (instantaneous voltage that must be exceeded by the noise for the repeater to

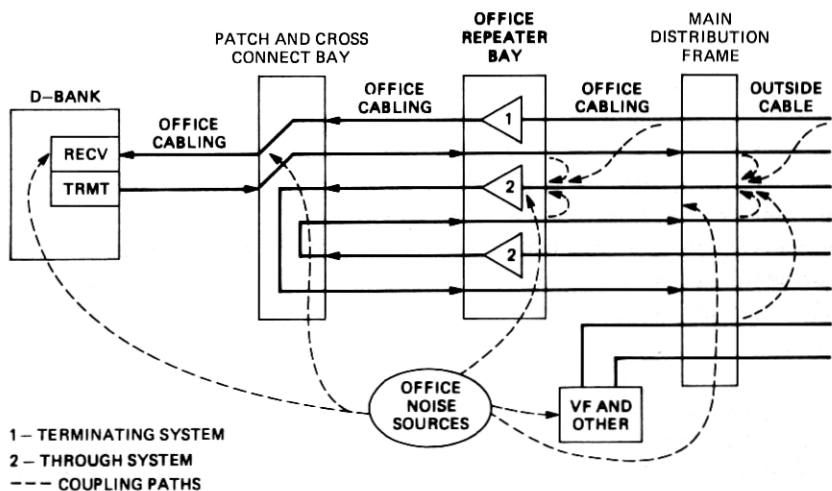


Fig. 9—Noise paths for end sections. Noise sources: cable crosstalk (from T1 and other services); frames, grounds, and power supply lines; radiative transmission; and unknowns.



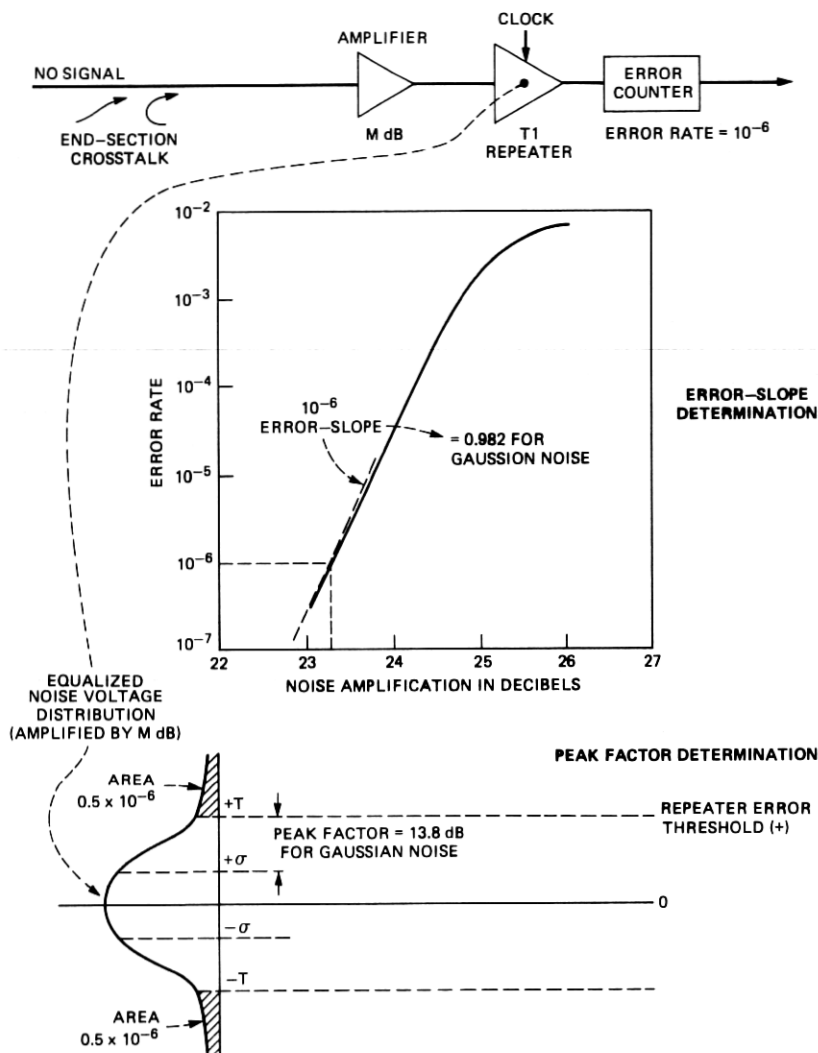


Fig. 10—End-section margin measurement for the 466/201 situation.

make errors) to the rms noise voltage which results in a  $10^{-6}$  error rate. The second parameter, error-rate slope, represents the change in the log of the error-rate-per-dB change of noise amplification at the repeater input, near the  $10^{-6}$  point (log of error rate = -6).

Both the peak factor and error-rate slope deviate predictably from the known values for a Gaussian-noise-amplitude distribution when impulses are present, or when a few disturbers ( $T1$  or periodic in nature) are dominant. The presence of impulses tends to lengthen the

tail of the noise-voltage distribution, thus, raising the noise peak factor and reducing the error-rate slope. The dominance of a single disturber sets a limit on the peak of the noise (truncates the noise-amplitude distribution), with consequent reduction of the peak factor and increase of the error-rate slope at the  $10^{-6}$  point. For example, the expected peak factor for Gaussian noise is about 13.8 dB, while the peak factor of the noise from a single T1 disturber (coupled through a FEXT path) is about 7 dB. The expected error-rate slope for Gaussian noise is 0.982, while Cravis and Crater (Ref. 2) measured slopes close to 0.1 (decades per dB) for office switching noise. See Fig. 10.

Figure 11 shows the distribution of peak factors observed in the end-section measurements. The mean value, 13.6 dB, indicates a slight tendency towards truncation, rather than impulses. However, about 15 percent of the lines show peak factors greater than 13.8, indicating impulsive effects. These points, however, were entirely from one measured cable, so that impulsive behavior was not the norm for the end sections measured.

Figure 12 shows the distribution of error-rate slope for all end sections measured. The mean slope, 1.0, indicates a tendency towards truncation of the noise distribution, in agreement with the peak factor results. The lower 15 percent of the distribution, indicating impulsive noise behavior, is again entirely due to the same particular end-section cable mentioned above.

In summary, noise on these central office pairs appears, overall, to be very nearly Gaussian in nature, with a slight tendency towards

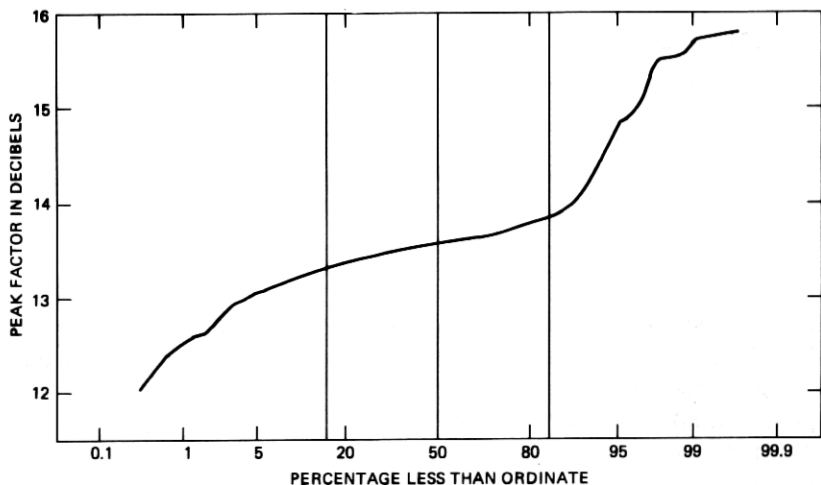


Fig. 11—End-section peak factors for the 466/201 situation. Number of points = 303; average = 13.6; standard deviation = 0.50.

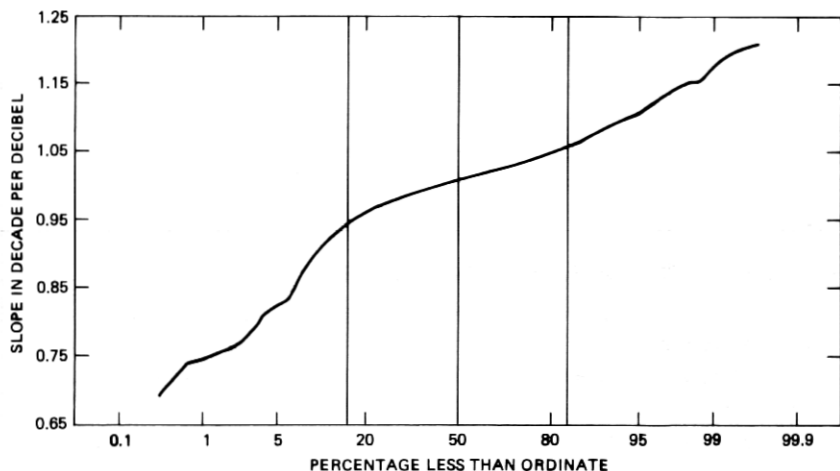


Fig. 12—End-section slopes for the 466/201 situation. Number of points = 300; average = 1.0; standard deviation = 0.08.

single-disturber effects (truncation). Only one cable was observed to have a noticeable impulsive noise background.

#### IV. ENGINEERING MODEL FOR T1 CARRIER

The performance objectives for individual T-carrier repeater sections depend on the maximum number of sections that are to be connected in tandem, as well as on the end-to-end performance objective for the complete T-carrier system. In metropolitan areas, where the maximum number of sections in tandem is expected to be 50, and where 95 percent of end-to-end systems must have error rates less than  $10^{-6}$ , the repeater-section objective can be stated: 99.9 percent of repeater sections must have error rates less than  $10^{-6}$ .

This objective is based on the assumption that the overall error rate of an end-to-end system is dominated by a single repeater section, such that the probability for the whole system of exceeding the specified error rate is the sum of the probabilities for each repeater section of exceeding the same error rate.

By definition, the margin of a repeater section that has an error rate of  $10^{-6}$  is zero, and the margin of a section with a smaller error rate is the amount of amplification of the noise at the repeater input that can be tolerated before an error rate of  $10^{-6}$  is reached. Since digital transmission systems are designed to have at least 3-dB reserve margin, the repeater-section objective can be stated: 99.9 percent of repeater sections must have margins better than 3 dB.

In other words, the margin at the lower 0.1-percent point of the repeater-section margin distribution must be greater than 3 db. The

margin distributions obtained from field measurements meet this objective with 4 to 6 dB to spare, as was shown in Fig. 2. If there is reserve margin in most of the T1 plant, it is conceivable that engineering rules could be modified, allowing more wire pairs in a cable to be reserved for use by the T-carrier. The following model may be used to predict the margin at the 0.1-percent point for various situations of cable-section layout and crosstalk noise.

#### 4.1 Factors affecting repeater-section margin

In a complete engineering analysis, one must be concerned with all of the following:

(i) Characteristics of the signal and noise sources (ones density of interfering T1 signals, mean time between impulsive events, etc.).

(ii) Amount and character of noise coupling (ACXT, FEXT, impulse noise, etc.).

(iii) Effects of system layout (cable loss, junctions) on both signal and noise.

(iv) Equalization properties of repeater (intersymbol interference and ALBO setting).

Most of the above elements are accounted for in the margin equation used for section engineering calculations.

#### 4.2 Margin equation

From the definition given above, a margin equation may be written

$$M = N(10^{-6}) - N(\text{actual}), \quad (1)$$

where  $M$  is the repeater-section margin in dB,  $N(10^{-6})$  is the average noise power in dBm at the repeater decision point (eye) which would produce an error rate of  $10^{-6}$ , and  $N(\text{actual})$  is the actual average noise power in dBm at the repeater eye for the given situation. It is assumed that the character of the noise (peak factor, spectral shape) in the first term above is identical to the actual noise encountered on the given repeater section, except for a flat gain.

The margin eq. (1), when applied to margin measurements involving noise amplification, also assumes that the noise appearing at the (internal) repeater decision point increases or decreases linearly with external amplification or attenuation at the repeater input. This assumption does not necessarily hold for repeaters with automatic gain adjustment (provided by an ALBO), since when the noise becomes a significant fraction of the signal voltage, the ALBO may be misled into assuming that a larger signal exists and reduce its gain accordingly. However, the adjustment of the margin equation (1) (by the addition of a new term to account for nonlinearity) is offset by a reduction in the peak signal power  $S$  (see below) by roughly the same amount so

that eqs. (1) and (2) may be used as given, if it is assumed that the repeater gain is always properly adjusted for the correct cable loss. (The above statement is true only for those repeaters for which the effective error threshold (noise voltage at which errors are made) is reduced by the same amount in dB that the ALBO gain has changed.)

For engineering analysis the margin equation may be broken up into five terms as follows:

$$M = (S - B - A) - (I + Q), \quad (2)$$

where

$$N(10^{-6}) = S - B - A, \text{ and } N(\text{actual}) = I + Q.$$

$S$  = the nominal peak signal power at the repeater decision point, which for the ideal T1 repeater equals 13.6 dBm. (See Section 4.6.)

$B$  = the ratio of peak signal voltage to rms noise voltage that would produce an error rate of  $10^{-6}$  with an ideal bipolar repeater, that is one with no intersymbol interference. For Gaussian noise, and assuming 50-percent ones density for the signal pulse stream,  $B = 19.7$  dB. (Note: this peak factor is defined slightly differently from the end-section peak factor of Section 3.2. It relates the rms noise level to the *peak signal* level, rather than to the error-threshold level. If the error threshold is set to one-half the peak signal height, then the difference in definitions amounts to 6 dB. The 0.1-dB residual difference between the end-section Gaussian peak factor 13.8 and the Gaussian value for  $B$ ,  $13.7 + 6.0$ , is because of the assumption of an "all zeroes" pulse stream for the end-section measurements, but a 50-percent ones density in the calculation of  $B$ .)

$A$  = the repeater degradation, an allowance for the nonideal performance of the repeater caused by intersymbol interference, threshold offsets, and jitter.  $A$  has traditionally been assigned a value of 6 dB in engineering calculations.<sup>2</sup> Empirical values for  $A$ , smaller than 6 dB, have been found in the present measurements.

Then,  $S - B - A$  is equal to the average noise power in dBm at the repeater decision point that will produce a  $10^{-6}$  error rate in a real repeater, where  $B$  depends on the characteristics of the noise present and  $A$  depends on the equalization properties and threshold setting of the particular repeater.

The actual (measured) noise power at the repeater decision point comprises two terms,  $I$  and  $Q$ , where:

$I$  = average noise power in dBm at the repeater decision point

which would be caused by a *single disturber* coupled through a *net coupling path loss* of 0 dB at 772 kHz. The "path" may include components from any or all of the ACXT, FEXT, or NEXT type.

$Q$  = scaling factor in dB which accounts for the fact that there are *many disturbers* of different types (ACXT, FEXT, NEXT) with a *distribution* of coupling path losses. As an "example," for ACXT alone,  $Q$  is the power sum of the apparatus-case slot-to-slot crosstalk coupling coefficients from all outputs (disturbers) into the slot being measured for margin.

$I + Q$ , called the *noise power sum*, is equal to the actual average noise power in dBm at the repeater decision point.

In Fig. 8, where the margin components (because of ACXT, FEXT, and NEXT) were separated, the coupling power sum,  $Q$ , was assumed to be the only variable. We will now investigate all terms in the margin eq. (2) to determine their actual variances as measured or derived in the field-measurement program.

#### 4.3 The noise power sum

In the field-measurement program, the average noise power ( $I + Q$ ) for all lines was measured directly in the absence of the T1 signal at the decision point of a test repeater, whose ALBO was held fixed to equalize for a particular length of cable (31.7-dB section loss at 772 kHz). Since the margin  $M$  is inversely related to the noise power ( $I + Q$ ) in the margin eq. (2), one expects a high degree of correlation between margin and noise power ( $I + Q$ ) from line to line, if the peak signal power  $S$ , noise peak factor  $B$ , and repeater degradation  $A$  do not vary appreciably from one line to the next.

A scatter plot of loss-adjusted\* test margin versus noise power is presented in Fig. 13. The solid line represents the best first-order fit to the data, where  $A_0$  and  $A_1$  are the intercept and slope of the fit. The dashed line represents the best fit with the slope constrained to  $-1.0$ , where  $B_0$  is the intercept obtained from the fit. The plot shows that the correlation between margin and noise power sum is almost dB for dB, with only a slight tendency towards increased margins at the low-margin (high-noise) end of the plot. The rms error in assuming a perfect one-to-one relationship between margin and noise power sum is 0.75 dB as indicated at the bottom of the plot; this may be considered to be the maximum error in assuming the other terms of the margin equation,  $S$ ,  $B$ , and  $A$  to be constants. (The actual error is less because

---

\* The margins are adjusted to the value they are expected to have for a section cable loss of 31.7 dB (at 772 kHz) which was the loss for which the fixed ALBO was set to equalize in the noise power measurements.

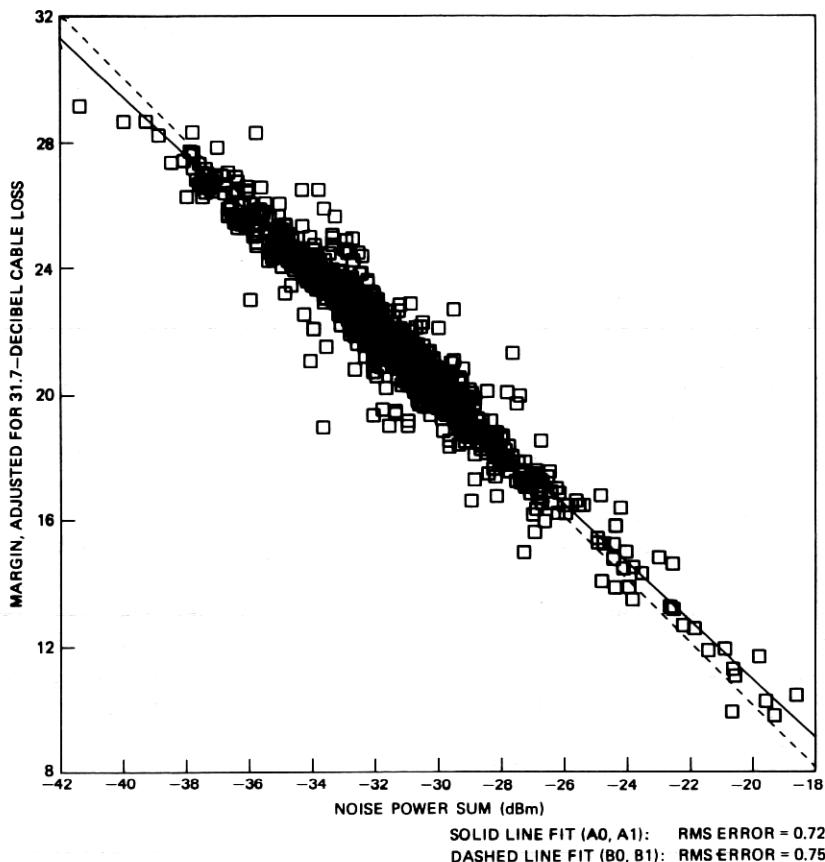


Fig. 13—Loss-adjusted test margins vs noise power sum for the 466/201 situation. Number of points = 850;  $A_0 = -7.60$ ;  $A_1 = 0.93$ ;  $R = 0.97$ ;  $B_0 = -9.86$ ;  $B_1 = 1.00$ .

the rms deviation on the scatter plot includes the effects of measurement error on margin, noise power, and cable loss.)

#### 4.4 The crosstalk coupling power sum

The coupling power sum is derived in Appendix B and is given by

$$q(l) = a_A + a_F(l)c(l, f_0) \quad (3)$$

and

$$Q = 10 \log_{10} q, \quad (4)$$

where the quantities (except  $l$ ) in (3) are power transfer ratios and

$a_A$  = the power sum of the ACXT crosstalk coupling coefficients from all disturbers.

$a_F(l)$  = the power sum of the equal-level FEXT crosstalk coupling coefficients for a section of length  $l$  from all disturbers.

$c(l, f_0)$  = the cable power transfer function at 772 kHz.

The following sections describe the distributions of  $a_A$  and  $a_F(l)$  found for the measured repeater sections.

#### 4.4.1 Apparatus case crosstalk

The ACXT power sum  $a_A$  was calculated for each measured line using eq. (23) of Appendix B. The distribution of  $a_A$  for the field measurements is shown in Fig. 14. Since apparatus-case crosstalk is dominant, the properties of this distribution are reflected into the properties of the distribution of repeater-section performance (margin). In particular, the bend observed in the ACXT distribution at the 5-percent point is directly reflected into a bend in the margin distribution at the same point, causing the worst margins to be lower than would be expected if a normal distribution were assumed with the measured values for the mean and standard deviation. The 6-dB slope of the low end of the ACXT distribution matches the 6-dB slope observed at the low end of the margin distribution (Fig. 2).

Of special interest is the 0.1-percent point of the distribution, where the repeater-section margin objective is defined. In the simplified margin model, where all parameters except  $Q$  are held constant, the value of  $Q_{ACXT}$  at the 0.1-percent point determines how much the T1 plant exceeds the section objective. The value at this point, determined by extrapolation of the trend of the high coupling end of the distribution, is about -55 dB, which translates to about 8.5 dB of margin for the measured sections in Fig. 8.

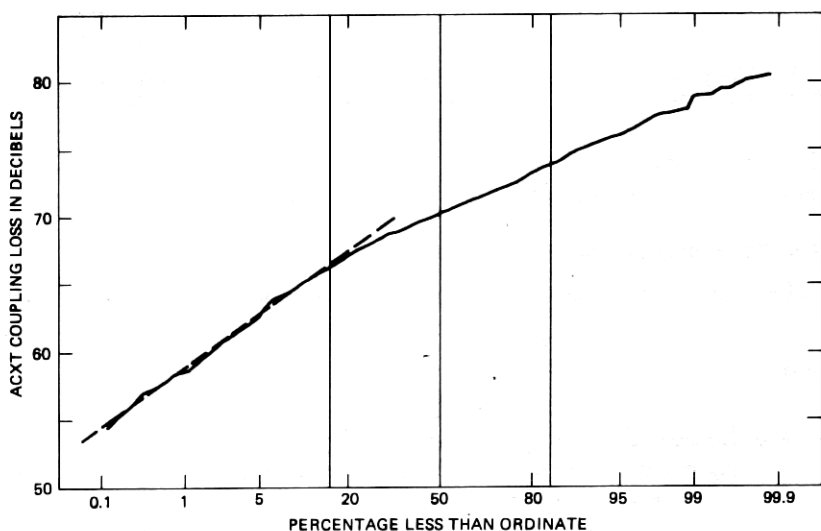


Fig. 14—ACXT power sum—all points measured for  $p$  and  $\alpha$ —for the 466/201 situation. Number of points = 8.0; average = -70.0; standard deviation = 3.94.



#### 4.4.2 Far-end crosstalk

The secondary source of crosstalk noise in the standard T1 system layout is FEXT occurring between cable pairs that have T1 signals travelling in the same direction and at equal levels. Coupling is most severe between pairs in the same binder group.

Far-end crosstalk power sums  $a_F(l)$  were calculated using eq. (24) in Appendix B. The distribution of  $a_F(l)$  for all lines is given in Fig. 15, where  $l$  is approximately 6000 feet.

The difficulties of separating ACXT and FEXT components of the noise for  $\alpha$ 's close to unity is illustrated by the turn-up of the distribution at high coupling losses (right side of Fig. 15). The error in the fit for  $\alpha$  is very high for these points and, therefore, they should be ignored in the characterization of the distribution properties.

Ignoring these points, the distribution may be roughly characterized as having a mean power sum of about 44.5 dB, with a standard deviation of about 2.5 dB. This is slightly less than the power sum mean for one cable measured directly for FEXT, for which the data (scaled to 772 kHz) are also plotted in Fig. 15. The standard deviation of the distribution of  $a_F$  is also slightly larger than that for the measured cable (1.5 dB). These differences imply less FEXT disturbers on average for the field measurements than for the laboratory-measured cable. However, the difficulties in calculating FEXT for different cable situations (different lengths, different splicing arrangements) make a meaningful comparison difficult.

The main distinguishing feature of the FEXT power sum distribution from the ACXT distribution is its smaller standard deviation, which

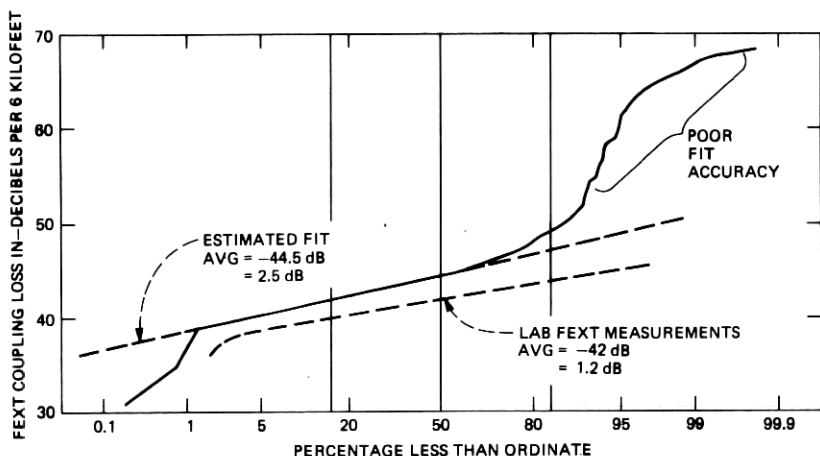


Fig. 15—FEXT coupling power sum for the 466/201 situation. Number of points = 514; average = 45.9; standard deviation = 5.68.

results from the greater number of noise sources and coupling points for FEXT. This lower standard deviation is reflected into the standard deviation of the upper end of the margin distribution (Fig. 2), where FEXT is strongest.

The predicted FEXT-alone margin distribution of Fig. 8, obtained from the  $\alpha_F$  distribution and the margin equation, shows that FEXT is only a secondary source of noise for a majority of the T1 plant.

#### 4.5 Single interferer noise power

By definition,  $I$  is the noise power at the repeater decision point attributable to a single interferer with 0-dB crosstalk coupling loss at 772 kHz.  $I$  depends on the spectral shape of the interferer's signal, the crosstalk coupling paths, the insertion loss of the line, and the repeater cable equalization. For the present analysis, the interferer's spectral shape is parameterized by  $p$ , the ones density, and the coupling path is parameterized by  $\alpha$ , the ratio of ACXT to total noise (ACXT + FEXT) at 772 kHz. From Appendix B, an expression for  $I$  is written:

$$I = 10 \log \left[ \int_0^\infty w(p, f) (f/f_0)^2 \left[ \alpha + (1 - \alpha) \frac{c(l, f)}{c(l, f_0)} \right] r(l, f) df \right], \quad (5)$$

where

$w(p, f)$  = the one-sided interferer's signal power spectrum, which depends on the ones density  $p$ .

$(f/f_0)^2 \left[ \alpha + (1 - \alpha) \frac{c(l, f)}{c(l, f_0)} \right]$  = the power transfer function of the crosstalk coupling path, which is defined to be 1 at  $f = f_0$ , and where  $c(l, f)$  is the power transfer function of the cable section of length  $l$  at frequency  $f$ .

$r(l, f)$  = the power transfer function of the repeater cable equalization where  $l$ , the length of the cable section, determines the overall amount of gain through the action of the ALBO.

##### 4.5.1 Dependence of $I$ on cable insertion loss

The dependence of section margin on cable insertion loss is entirely through the  $I$  term of the margin eq. (2). The insertion loss power ratio  $1/c(l, f)$  appears in both the repeater gain shape and in the FEXT part of the crosstalk coupling expression. For ACXT-dominated lines,  $I$  decreases by about 1.09 dB for every dB increase in insertion loss at

772 kHz. This is entirely through the action of the ALBO acting to change the overall gain of the repeater to bring the equalized signal up to a given peak level. The field measurements allowed the calculation of the quantity  $I(L) - I(L_0)$  for each line measured, where  $L$  was the measured insertion loss in dB for the given line and  $L_0$  is equal to 31.7 dB, which was the loss equalized for by the test repeater for all noise power measurements. This quantity eliminates the large variation in  $I$  for a given loss due to variation in  $Q$  over the lines measured. It is plotted versus measured insertion loss in Fig. 16. The one-for-one dependence of  $I$  on insertion loss is clearly seen.

#### 4.5.2 Dependence of $I$ on $p$ and $\alpha$

The single interferer noise power  $I$  also depends on the ones density of the interferer and on the fraction of interference due to ACXT and FEXT. A plot of  $I$  versus  $p$  for  $\alpha = 0, 0.5$ , and 1 calculated for the test

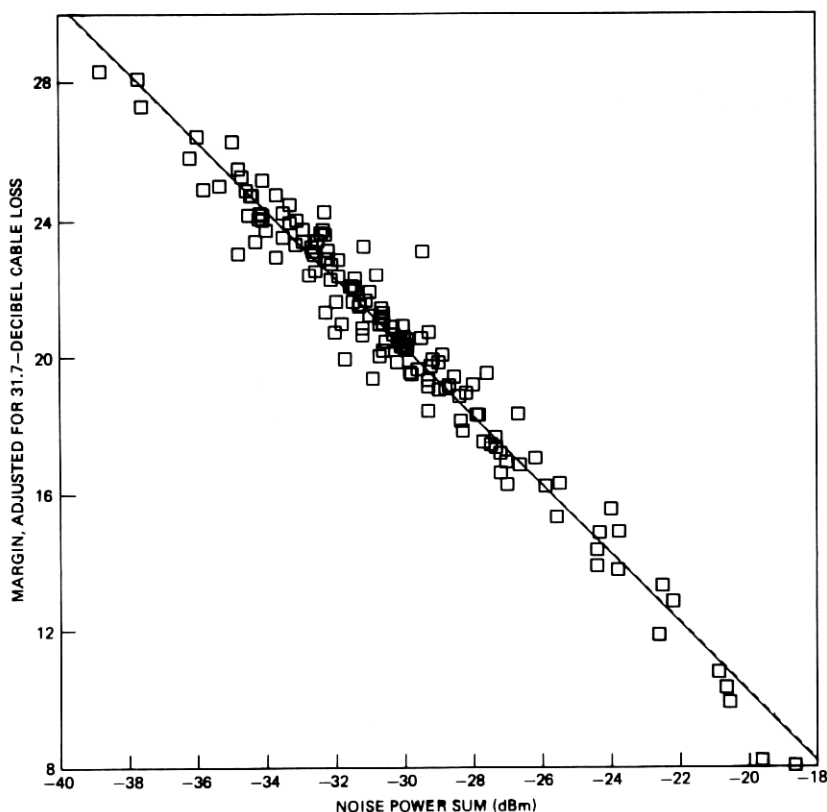


Fig. 16—Relative noise power integral vs. insertion loss for the 466/201 situation. Measurements relative to  $L = 31.7$  dB. Number of points = 864;  $A_0 = -33.56$ ;  $A_1 = 1.05$ ;  $R = 0.90$ .

repeater for a 772-kHz section loss of 30.7 dB is given in Fig. 17. (The value of  $I$  for the theoretical 100-percent cosine roll-off repeater defined by eqs. (19) and (22) ranges about 1.5 to 3.0 dB greater than the equivalent value of  $I$  for the test repeater.)

The ones density dependence reflects the fact that as more pulses are sent on the disturbers, more crosstalk power is generated. Roughly speaking, twice the pulse density on the disturbers will produce twice the noise power (3-dB increase), except where adjacent pulse interference or coherent effects over several disturbers cause a large degree of cancellation or reinforcement.

The change of  $I$  with change in  $\alpha$  is small and may be positive or negative depending on the repeater preamplifier gain shape. For example,  $I$  increases by about 0.6 dB for the theoretical 100-percent cosine roll-off repeater when  $\alpha$  changes from 0 to 1. However,  $I$  decreases by 0.7 dB for the test repeater for the same change in  $\alpha$ .

#### 4.6 Peak signal power at the repeater decision point

For an ideal repeater, which perfectly equalizes the cable-loss shape, the T1 signal spectrum is operated on by a 100-percent cosine roll-off low-pass filter with compensation for 50-percent duty cycle pulses as shown in eq. (19). The overall gain at the midpoint of the roll-off

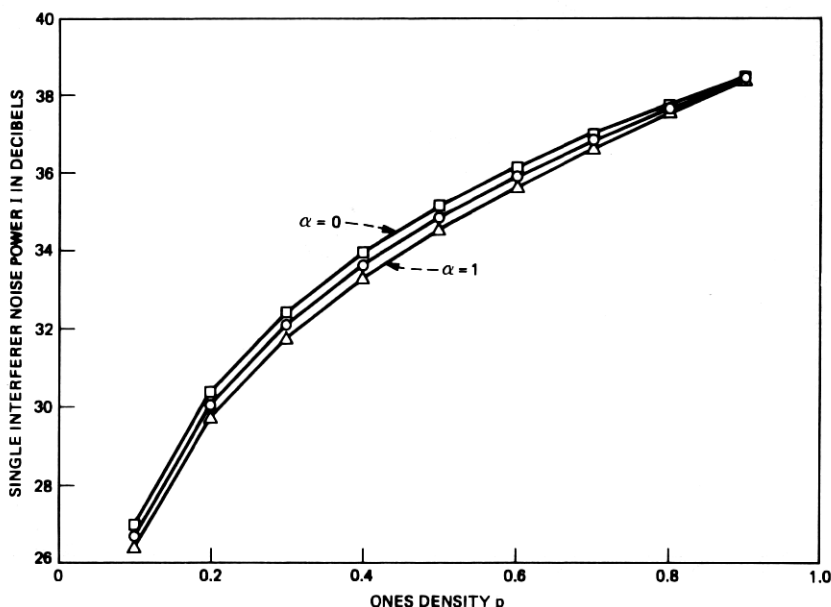


Fig. 17—Single interferer noise power vs.  $p$  and  $\alpha$  measured for the test repeater—772-kHz loss = 30.7 dB.

function is  $-6.0 + 0.91$  dB, where the second term is an adjustment for 50-percent duty-cycle pulses. Since the power of a 3-volt, 50-percent duty cycle, all ones T1 signal at 772 kHz is 18.7 dBm, the peak power at the repeater decision point may be estimated as  $18.7 - 6.0 + 0.9 = 13.6$  dBm.

#### 4.7 Peak signal-to-rms-noise ratio

The term  $B$  is defined as the ratio of the peak signal voltage to the rms noise voltage that would produce a  $10^{-6}$  error rate in an ideal repeater.  $B$  will change depending on the ones density of the line being measured, since the probability of error given a zero (no pulse) is not necessarily equal to the probability of error given a one (positive or negative pulse). For Gaussian noise,  $B$  is 19.6 dB, assuming all ones, or 19.7 dB, assuming 50-percent ones, where the error threshold is assumed to be exactly one-half the peak equalized pulse height. Since the average ones density observed in the field measurements was about 0.7, we will, in general, assume the Gaussian peak signal-to-rms-noise ratio to be about 19.7 dB.

$B$  was calculated for a subset of lines for which noise voltage distribution measurements were made in the field. This subset was not random, and tended to emphasize those lines that had low margins or obvious single disturber effects, as seen by a visual inspection of the crosstalk noise at the repeater decision point. The resultant distribution of  $B$  is plotted in Fig. 18.

The average value of  $B$  calculated for the selected lines was 19.3 dB,

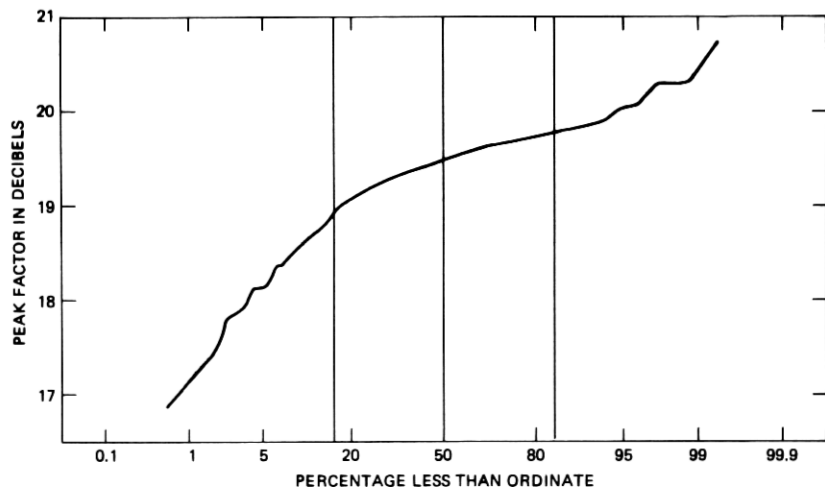


Fig. 18—Peak factor for the 466/201 situation. Number of points = 165; average = 19.3; standard deviation = 0.56.

quite close to the Gaussian value. The lowest value determined for  $B$  was about 17 dB, which is closer to the Gaussian value than the value expected for a single T1 disturber (13 dB for FEXT).

A slight correlation of peak signal-to-rms-noise ratio with margin has been observed such that the lowest margins are increased by a small amount (by about 0.7 dB on average) over what would be expected if the noise were Gaussian with the same rms voltage, as assumed in the simplified model of Section III. This effect is shown in Fig. 13 by the fact that the best fit to the margin versus noise power data (solid line) has a slope less than one (dashed line), and that the fitted curve is about 0.7 dB above the unit-slope curve at the low-margin end. That the correction for peak factor indeed reduces this discrepancy is illustrated in Fig. 19, which shows the same plot as Fig. 13 (but only for those lines for which  $B$  was measured), except that the

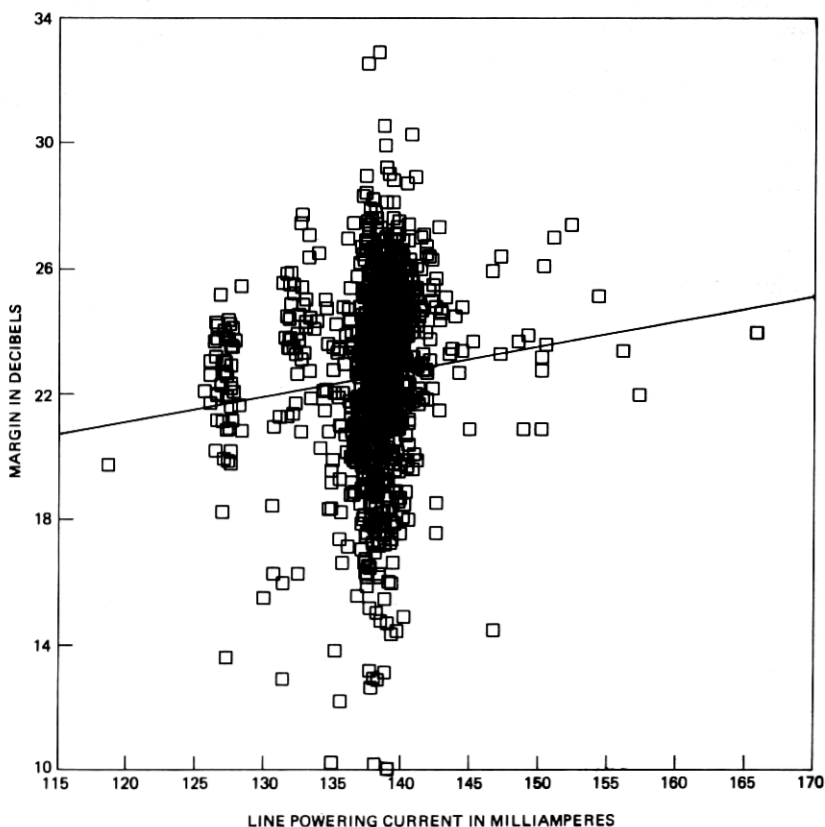


Fig. 19—Loss-adjusted test margin vs. power sum for the 466/201 situation. Number of points = 144;  $A_0 = -9.89$ ;  $A_1 = -1.00$ ;  $R = 0.98$ ;  $B_0 = -9.77$ ;  $B_1 = -1.00$ .

margins have been corrected to a constant value for  $B$ . The coincidence of the fitted and unit-slope lines is almost exact.

The main reason for the reduction of  $B$  for low-margin lines appears to be that apparatus-case crosstalk is controlled by within-slot coupling. With only one or two disturbers, the noise-amplitude distribution is truncated, and the peak factor is reduced. The reduction is quite small, however, and even in situations where one noise source was observed to be visually dominant at the repeater decision point, only a slight reduction of peak factor from Gaussian was seen, indicating that residual noise was present.

#### 4.8 Repeater impairment

The value of  $A$ , the repeater impairment, is defined by the margin eq. to equal:

$$A = S - B - (I + Q) - M, \quad (6)$$

where  $S = 13.6$  dBm and  $M$  and  $(I + Q)$  are measured. The value of  $B$ , the peak signal-to-rms-noise ratio at a  $10^{-6}$  error rate, is less well determined, since voltage-distribution measurements were made on only a small subset of the total lines measured.

If we assume the mean measured value, 19.3 dB, for  $B$ , we obtain a distribution for  $A$  for the test repeater as shown in Fig. 20. The distribution of calculated  $A$  values for the test repeater runs from 2 to 9 dB, a fairly large range. Other than variations caused by differences in cable loss versus frequency shape from pair to pair (resulting in differences in equalization from line to line, even with the same

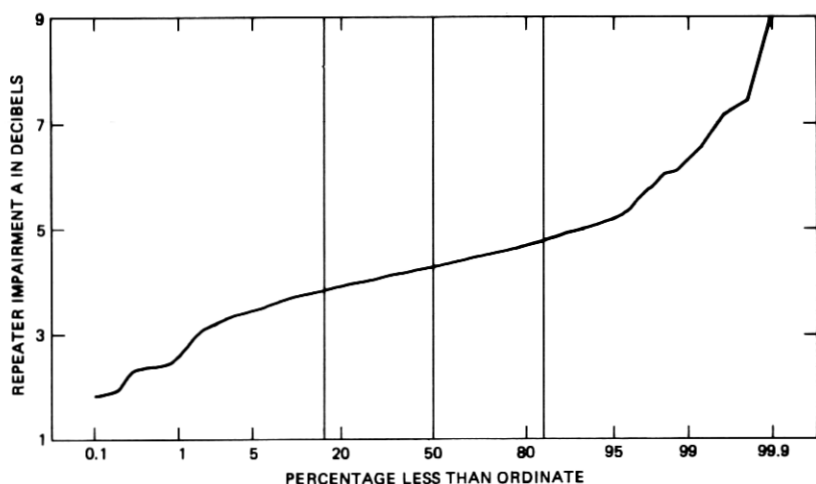


Fig. 20—Repeater impairment for the 466/201 situation. Number of points = 962; average = 4.31; standard deviation = 0.61.

repeater), one expects the degradation  $A$  for a given repeater to be constant. Indeed, although the extreme ends of the measured distribution of  $A$  are widely separated, 95 percent of the points lie between 3 and 6 dB, resulting in an overall standard deviation of only 0.61 dB about the mean of 4.3. Much of the variation is likely because of measurement error for the margin  $M$  and the noise power sum ( $I + Q$ ), as well as the fact that the  $A$  values are uncorrected for variations in  $B$ .

The expected  $A$  for the ensemble of service repeaters measured in the field may be related to the differences in margin observed between test and service repeaters. The distribution of test-minus-service margin is plotted in Fig. 21. The mean difference is  $-0.2$  dB, indicating the average service-repeater performance was slightly better than the test-repeater performance. The standard deviation of test-minus-service difference is 0.91 dB, indicating corresponding variation in repeater properties (equalization gain shape, threshold offsets, etc.).

Since the distribution of test-minus-service margin has a mean near zero for the field measurements, the expected  $A$  value for service repeaters is also 4.3 dB, if one assumes the average  $I$  value (which depends on the repeater gain shape) to be the same for test and service repeaters. If  $I$  is not the same, then at best we know that the quantity ( $I + A$ ), which is a measure of the overall repeater performance, is the same on the average for the test and service repeaters.

Since the 4.3 dB value for  $A$  is 1.7 dB less than has been previously assumed for section engineering,<sup>2</sup> and the value of  $I$  for the test repeater is 1.5 to 3.0 dB less than  $I$  for the 100-percent cosine roll-off repeater, which has been used in the past for system engineering, the

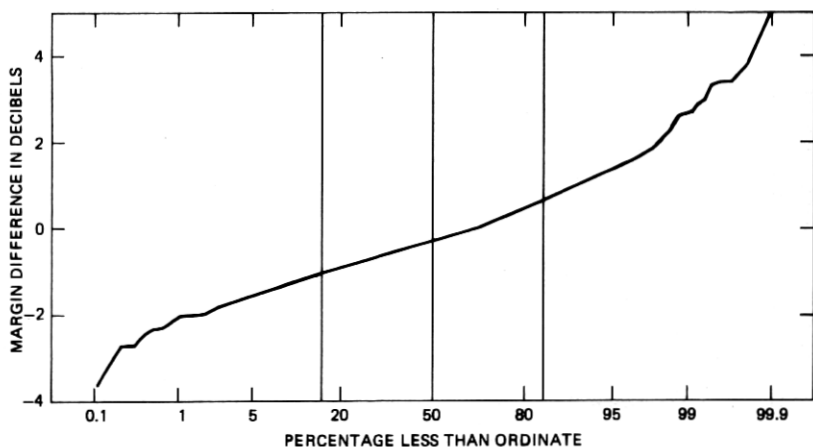


Fig. 21—Test-minus-service repeater margin for the 466/201 situation. Number of points: 913; average  $0 = -0.20$ ; standard deviation = 0.91.



overall repeater performance observed in the field averages about 4.0 dB better than has been previously assumed.

#### **4.9 Summary of margin model as applied to field measurements**

The margin eq. (2) has been used to account for the margin performance of intermediate-repeater sections of known cable loss  $L$ , in a noise environment characterized by peak signal-to-rms-noise ratio  $B$ , effective disturber ones density  $p$ , fraction apparatus-case crosstalk  $\alpha$ , and total equalized noise power  $(I + Q)$ . The independent measurement or calculation of these quantities, along with the measurement of actual margin itself allowed the determination of a value for the repeater degradation  $A$  for the test repeater, and by inference, limits on  $A$  for the population of service repeaters in the field.

Since the range of variation of the parameters  $L$ ,  $A$ , and  $B$  was very small for the particular set of lines measured (e.g. almost all lines were 6 kft long), it was possible to obtain a very good fit to the measured margin distribution by setting  $L$ ,  $A$ , and  $B$  to their mean values and assuming that the crosstalk coupling power sum  $Q$  was the only random variable from line to line. The distribution of  $Q$  then mapped directly onto the distribution of  $M$ .

However, it is desirable to go beyond the limited set of repeater-section layouts studied in the field measurements. If the total population of T1 repeater sections is to be considered, values for model parameters, especially section-loss  $L$ , must be taken from distributions of all possible values in order to predict current performance, or must be taken from expected extreme limits in the engineering of sections to perform properly under all conditions.

### **V. ADDITIONAL CHARACTERIZATION RESULTS**

Measurements of basic cable and system parameters (such as insertion loss and dc powering current) and of margins for less common or nonstandard situations were made in the field-measurement program. Some of the results are described in this section.

#### **5.1 Cable insertion loss**

The insertion loss of each cable section measured has a direct impact on the margin expected for the section, mainly because the amount of signal attenuation is the main determining factor of the expected signal-to-noise ratio at the receiving repeater input.

Figure 22 is a plot of the distributions of cable-section insertion loss at 772 kHz for all of the 22-gauge pulp sections measured for margin. The different average section losses reflect the different section lengths. The standard deviation of loss about the mean is approximately the same for all sections measured and is about 0.5 dB. This

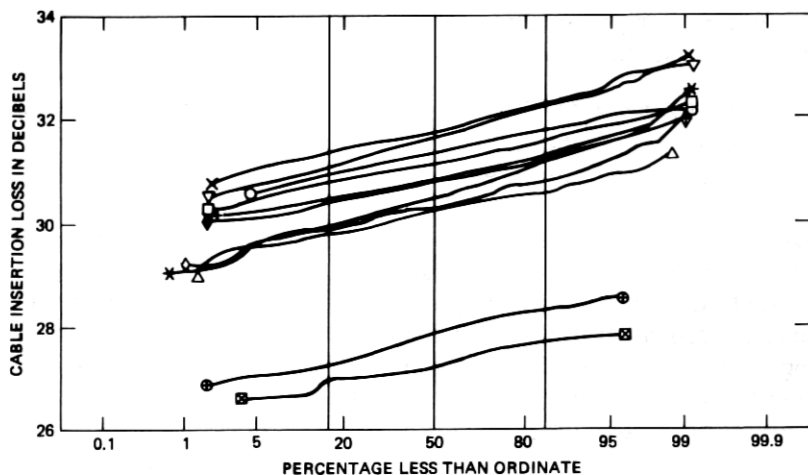


Fig. 22—Distributions of 772-kHz insertion loss showing separate results for each cable for the 466/201 situation. Number of points = 923.

variation is reflected into an expected variation of service margins for each section, which, however, is usually not directly apparent since variations due to crosstalk noise differences from line to line predominate over variations due to differences in insertion loss.

If insertion losses are normalized to 1 kft, the distribution of losses in dB per kft of Fig. 23 is obtained. The mean result, slightly less than 5.2 dB per kft, is in agreement with the 772-kHz losses of previous measurements of 22-gauge pulp cable.

## 5.2 Dc simplex powering current

One of the measures of system integrity is the dc current used to power the manhole repeaters. This current is sent in simplex mode (longitudinally over the same wire pair used for the signal) from one of the span offices through all the side-1 regenerators, is looped back at some intermediate point or at the other span office, and returns to the original office through all the side-2 regenerators of the given line.

The nominal value for this current is 140 mA dc for the older repeater types. Figure 24 shows the distribution of observed currents for the repeater sections that were measured for margin. While the mean is close to the nominal value, some outliers are strongly apparent. (The set of points at about 125 mA all come from the same span.) However, the repeater powering voltage is not strongly dependent on the line powering current, and therefore, most repeaters will operate without observable margin degradation over a wide range of current. A scatter plot of margin versus powering current, Fig. 25, shows no obvious correlation; however, since the margin variations are domi-

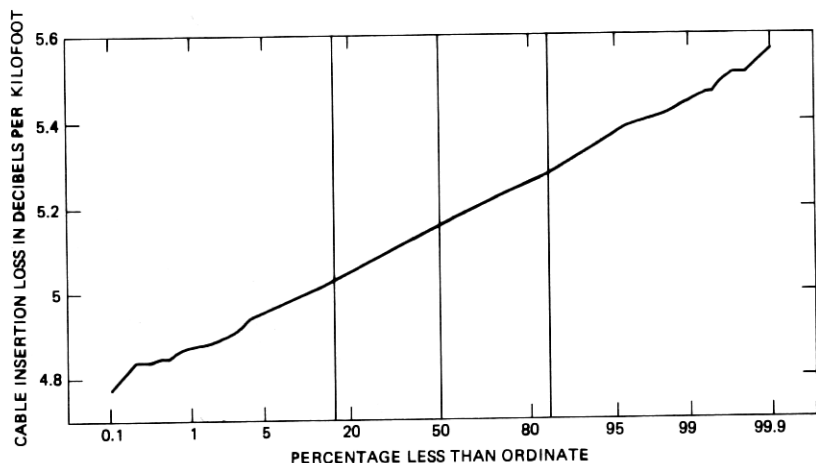


Fig. 23—Distributions of 772-kHz insertion loss in dB/kft for the 466/201 situation. Number of points = 923; average = 5.16; standard deviation = 0.12.

nated by crosstalk noise variations, small correlations between margin and powering current are not easily observed.

### 5.3 Other margin measurements

While we have concentrated on a “standard” configuration of 22-gauge pulp cable with 466-type apparatus cases and 201-type repeaters, it is important to note that a significant fraction of the physical plant does not have this configuration. Perhaps the most common difference are the use of lightning-protected 205-type repeaters in 468-type ap-

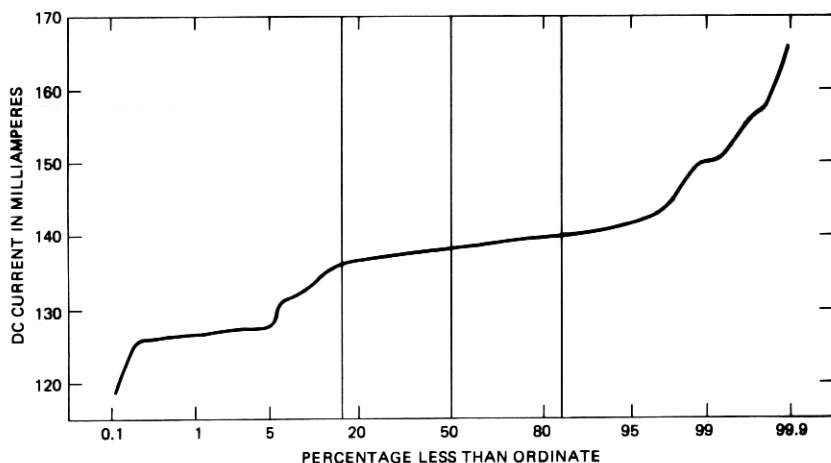


Fig. 24—Line-powering currents for the 466/201 situation.

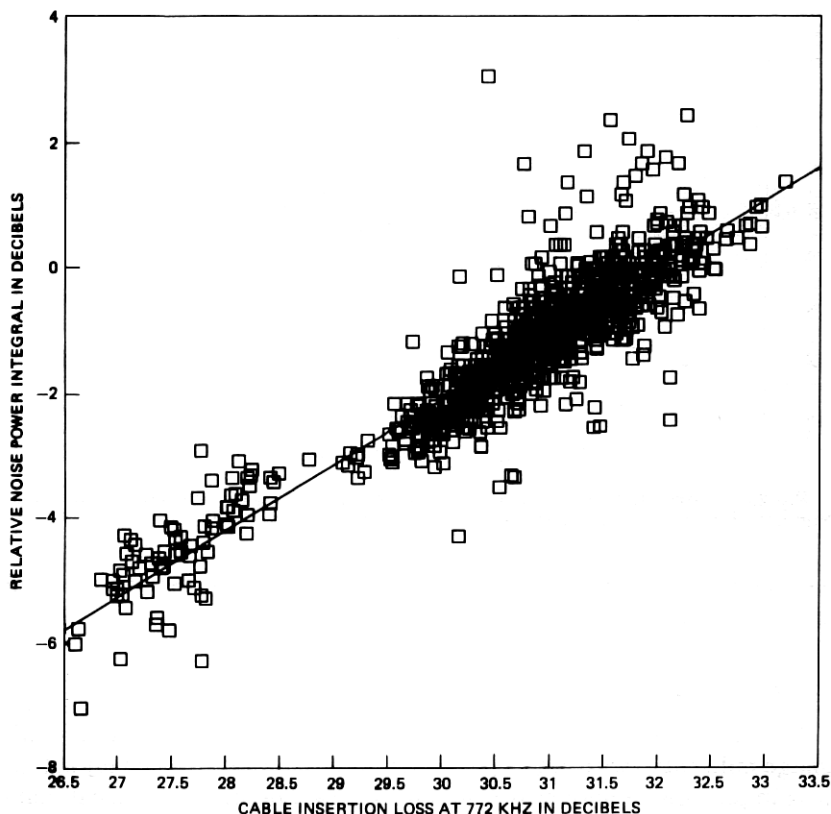


Fig. 25—Margin vs. line-powering current for the 466/201 situation. Number of points = 922; average = 137.9; standard deviation = 3.85.

paratus cases, and the deployment of the newer and smaller 208- and 209-type integrated circuit repeaters in the 475-type apparatus case. Also, the use of 19- and 24-gauge instead of 22-gauge and the use of polyethylene-insulated conductor (PIC) instead of pulp insulated cable is not uncommon. A relatively small subset of field measurements treated some of these “nonstandard” situations.

### 5.3.1 Apparatus case type 475

About one sixth of the lines measured for margin had 475-type apparatus cases rather than the more usual (for these measurements) 466-type. These cases house the 208- or 209-type integrated circuit repeater. A comparison of case performance may be made by observing margins measured using the test repeater for both case types.

Figure 26 shows the measured margin distributions for the test repeater for the two types of cases. The mean margin for the 475 distribution is about 1 dB worse than the mean 466 margin. However,

differences in FEXT contributions for the two measurement groups are responsible for at least part of this difference.

The lower portions of the two distributions, most likely dominated by ACXT effects, have estimated asymptotes indicated by the straight lines shown. Although the data available for the 475 cases are small, it appears that they may be treated equivalently to 466 cases in margin calculations, since the estimated effects at the 0.1-percent point are the same.

### 5.3.2 Nineteen-gauge cable, NEXT exposure

One of the special conditions encountered in the field measurements was a single 455-pair 19-gauge pulp cable using 22-gauge section lengths, which was completely filled with T-carrier so that opposite directions of transmission sometimes appeared in adjacent binder groups. This configuration made cable NEXT the dominant source of noise at the repeater input, at least for those binder groups that were adjacent to T1 groups with transmission in the opposite direction.

Figure 27 shows the measured distributions of test repeater margins for each of the six binder groups observed for this cable. The lowest margins occur for binder groups in the outer part of the cable, where adjacent-unit NEXT was dominant. The next lowest margins occurred for inner binder groups that were subject to adjacent- or alternate-unit NEXT from other inner or outer binder groups. The best margin distribution was observed for a binder group that had no adjacent-unit NEXT exposure.

The situation illustrates the engineering tradeoff between number

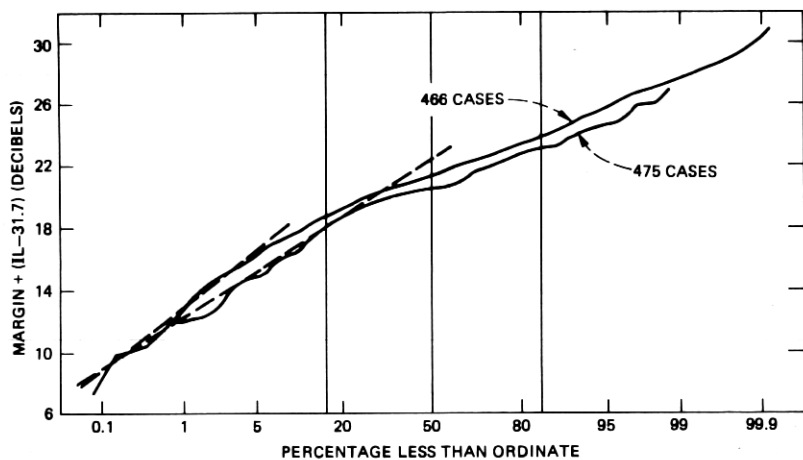


Fig. 26—Test margins (loss corrected) for the 466 and 475 apparatus cases. Number of points = 1401;  $A_0 = 11.47$ ;  $A_1 = 0.08$ ;  $R = 0.10$ .

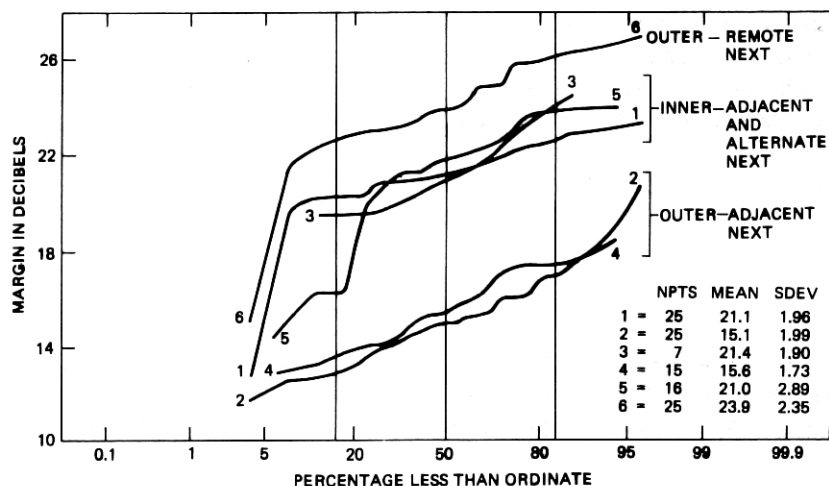


Fig. 27—Test margins for a 23-dB loss cable section with adjacent-unit NEXT. Number of points = 113.

of systems allowed in the cable and repeater section transmission loss. About twice the usual number of systems have been allowed in the cable (thus, raising levels of NEXT), while the section loss has been held to about 23 dB (by using 22-gauge section lengths for 19-gauge cable). Also illustrated is the fact that outer binder groups are more susceptible to adjacent-unit NEXT coupling (especially from other outer binder groups) than are inner binder groups.

## VI. SUMMARY

The measurement program described here has provided data on about 2000 T1 intermediate repeater section lines most of which are operating in the 466/468 apparatus-case environment. The principal results of this program are as follows:

(i) The average margin observed for T1 repeater sections (whose average cable insertion loss is 30.7 dB at 772 kHz) is 22.6 dB. The estimated margin at the 0.1-percent point of the distribution is 8.5 dB. These results imply that for properly engineered systems, almost no errors should result from intersystem crosstalk.

(ii) Repeater section margin at  $10^{-6}$  error rate may be accurately predicted if the crosstalk noise power sum at the decision point of the T-carrier repeater is known. Other parameters, such as repeater degradation A, or noise peak factor B, may be held to constant (average) values in the prediction of margin.

(iii) Apparatus-case crosstalk is the dominant form of crosstalk interference for intermediate sections where 466, 468, and 475 cases are used. 80 percent of lines have more crosstalk energy at 772 kHz

from ACXT than from FEXT; about 5 percent of lines show no FEXT at all ( $\alpha = 1$ ).

(iv) The average repeater performance ( $I + A$ ) observed in the field measurements is about 4 dB better than has been previously assumed in models featuring the 100-percent cosine roll-off transmission channel. The single interferer noise power  $I$  is 1.5 to 3.0 dB less for a specific test repeater than for the 100-percent cosine roll-off repeater, and the repeater degradation  $A$  for the practical repeater is 1.7 dB less than has been previously assumed in the engineering model.

(v) The mean peak factor determined for intersystem crosstalk noise is about 19.3 dB, very close to the Gaussian value of 19.7. The peak factors for low margin lines are about 0.7 dB less than the average, thereby raising the margins of these lines about 0.7 dB above that expected from knowledge of only crosstalk noise power and the average peak factor. Most end sections exhibited very nearly Gaussian noise; a few did show evidence of noise that was impulsive in nature (high peak factors).

## VII. ACKNOWLEDGMENTS

The authors appreciate the help and cooperation given by the management, office craftspeople, and outside plant technicians of the Bell System operating companies in which the field measurements were performed. The contributions to the field-measurement program and subsequent analysis by the members of digital transmission groups at Bell Laboratories in West Long Branch, N. J., as well as discussions with members of interested groups at Bell Laboratories in Holmdel, N. J. and in Merrimack Valley, Mass. are gratefully appreciated.

## APPENDIX A

### ACXT and FEXT Components of Margin

The predicted margin curves of Section III were calculated from the margin equation (2), assuming constant values for all terms except  $Q$ , the power sum of the crosstalk coupling coefficients. The following values were used:

$$S = 13.6 \text{ dBm}$$

$$B = 19.3 \text{ dB}$$

$$A = 4.3 \text{ dB}$$

$$p = 0.69$$

$$\alpha = 0.69$$

$$L = 30.7 \text{ dB}$$

$$I(p, \alpha, L) = 36.53 \text{ (ACXT)}$$

$$I(p, \alpha, L) = 37.04 \text{ (FEXT)}$$

$$I(p, \alpha, L) = 36.45 \text{ (NEXT)}$$

The values for  $I$  were obtained by applying eq. (5) to the test repeater used in the margin measurements. Results for ACXT and FEXT are plotted in Fig. 17. For the NEXT value for  $I$ , eq. (5) was used except the  $(f/f_0)$  dependence was changed from squared to the power 1.5, characteristic of NEXT.

Then the margin equations for ACXT, FEXT, and NEXT become:

$$M_{ACXT} = -46.59 - Q_{ACXT} \quad (7)$$

$$M_{FEXT} = -47.10 - Q_{FEXT} \quad (8)$$

$$M_{NEXT} = -46.51 - Q_{NEXT} \quad (9)$$

Using the values for  $Q$  derived from Figs. 2 and 3, the predicted margin curves in Section III for ACXT and FEXT were obtained.  $Q_{ACXT}$  and  $Q_{FEXT}$  were obtained using eqs. (23) and (24) in Appendix B. The distribution of  $Q_{NEXT}$  was obtained by assuming average alternate unit NEXT pair-to-pair coupling averaging  $-103$  dB with standard deviation of 7 dB and assuming 50 alternate-unit disturbers.<sup>2</sup> The average power sum  $Q_{NEXT}$  for this situation is  $-80$  dB with standard deviation 2.0 dB. Applying this to eq. (22) produces the predicted NEXT margin curve of Fig. 8.

## APPENDIX B

### ACXT and FEXT Components of Noise

Assuming that NEXT is negligible, the noise power density (watts/Hz) at the repeater input (before equalization) because of a single T1 disturber may be broken down into ACXT and FEXT components as defined in the equation:

$$n(p, l, f) = w(p, f)[x_A(f) + x_F(l, f)c(l, f)], \quad (10)$$

where all terms represent single-sided power spectral densities, and it has been assumed that ACXT and FEXT signals are independent so that their powers may be added directly to produce the total noise power.

(i)  $w(p, f)$  is the power spectral density of the T1 signal at the disturber source (repeater output) where  $p$  is the ones density. It is given by:

$$w(p, f) = \frac{2A^2}{R} \frac{T}{2} p(1-p) \cdot \left[ \frac{\sin \pi f T / 2}{\pi f T / 2} \right]^2 \frac{1 - \cos(2\pi f T)}{1 + 2(2p - 1)\cos(2\pi f T) + (2p - 1)^2}. \quad (11)$$

This represents a bipolar pulse stream with ones density  $p$ , rectangular pulses with 50-percent duty cycle, pulse period  $T$ , pulse amplitude  $A$ , through a reference impedance  $R$ . For T1 systems,  $1/T = 1.544 \times 10^6$  Hertz,  $A = 3$  volts, and  $R = 100$  ohms.



(ii)  $x_A(f)$  is the crosstalk power transfer function from disturber source to test-repeater input, where the disturber source is located in the same apparatus case as the test repeater.

(iii)  $x_F(l, f)c(l, f)$  is the crosstalk power transfer function from disturber source to test repeater input where the disturber source is located at the opposite end of the repeater section from the test repeater and couples through FEXT paths in the main cable. A factor  $c(l, f)$ , representing the cable (power) transfer function, i.e. the inverse of the cable loss, has been split off to separate crosstalk effects from cable propagation effects. The factor  $x_F(l, f)$  represents the equal-level FEXT coupling (power) transfer function for a cable section of length  $l$ . The dependence on  $l$  is different for different cable types and splicing arrangements. Pulp cable and random splicing result in a tendency for power addition of FEXT noise currents generated along the length of the cable, while PIC cable and color-for-color splicing result in a tendency for voltage addition.

The expression for the noise power density, caused by multiple disturbers, is a sum of terms  $n(p, l, f)$  for each disturber, assuming independence of disturber signal sources. If all disturbers have a ones density  $p$ , then eq. (10) may be used to describe the total noise at the repeater input, provided that we interpret  $x_A(f)$  and  $x_F(l, f)$  as *power sums* of the individual pair-to-pair coupling coefficients.

We can simplify the expression (10) by assuming a common dependence on frequency  $f$  of the coupling power sums:

$$x_A(f) = a_A(f/f_0)^2 \quad x_F(l, f) = a_F(l)(f/f_0)^2, \quad (12)$$

where  $f_0$  is the one-half baud for T1, 772 kHz. This gives:

$$n(p, l, f) = w(p, f)(f/f_0)^2[a_A + a_F(l)c(l, f)]. \quad (13)$$

Finally, we can parameterize the relationship between ACXT and FEXT by defining:

$$\alpha = \frac{a_A}{a_A + a_F(l)c(l, f_0)}, \quad (14)$$

where  $\alpha$  represents the fraction of the noise density at  $f = f_0$  that is caused by apparatus-case crosstalk. (Note, this is *not* the same as the fraction of total integrated noise power due to ACXT.) The noise power density at the repeater input may then be expressed:

$$n(p, \alpha, l, f) = w(p, f)(f/f_0)^2 q(l) \left[ \alpha + (1 - \alpha) \frac{c(l, f)}{c(l, f_0)} \right], \quad (15)$$

where

$$q(l) = a_A + a_F(l)c(l, f_0). \quad (16)$$

Since, at  $f = f_0$ , eq. (15) reduces to

$$n(p, \alpha, l, f_0) = w(p, f_0)q(l), \quad (17)$$

then  $q(l)$  is the power sum, from all sources, of the crosstalk coupling coefficients at  $f = f_0$  to the repeater input of the line being tested.

Equation (15) is a function of the frequency  $f$ , and of the parameters  $p$ ,  $\alpha$ , and  $l$ . Direct measurements were made of the *relative* value of  $n(p, \alpha, l, f)$  for 3 to 5 frequencies for each T1 line. Since the cable loss  $1/c(l, f_0)$  was also measured, the parameters  $p$  and  $\alpha$  could be determined by fitting the equation (15) to the data, where the frequency dependence of the dB cable loss was assumed to be  $f^{0.58}$ , as was measured for the pulp cables surveyed in these field measurements.

The interpretation of the value obtained for  $p$  in the fit is slightly ambiguous, because it is known that all disturbers did not have the same ones density. However, the parameter  $p$ , redefined as some sort of *composite ones density* for all the disturbers, was quite useful in characterizing the noise, and behaved in a reasonable manner as discussed in the main body of the text.

The total noise power appearing at the decision point of the repeater (i.e. after equalization) is given by:

$$n_{\text{tot}}(p, \alpha, l) = \int_0^\infty n(p, \alpha, l, f)r(f)df, \quad (18)$$

where  $r(f)$  is the (power) gain of the repeater input equalization. Note, the repeater input gain normally depends also on the cable loss  $1/c(l, f_0)$  through the action of the ALBO in restoring a T1 signal to fixed equalized pulse height. However, for noise measurements, the ALBO was disabled and the repeater gain fixed to equalize a fixed cable loss (31.7 dB) at 772 kHz. For an ideal repeater with 100 percent cosine roll-off, and compensation for 50-percent duty cycle pulses, the gain is given by:

$$[r(l, f)]^{1/2} = \frac{1}{2} \left[ 1 - \sin\left(\frac{\pi f - f_0}{2 f_0}\right) \right] \left( \frac{\pi f / 4 f_0}{\sin \pi f / 4 f_0} \right) \frac{1}{[c(l, f)]^{1/2}} \quad (19)$$

for  $|f| \leq 2f_0$  and equals zero otherwise.

Substituting from eq. (15) into eq. (18), the total noise power at the repeater decision point is:

$$n_{\text{tot}}(p, \alpha, l) = q(l) \int_0^\infty w(p, f)(f/f_0)^2 \cdot \left[ \alpha + (1 - \alpha) \frac{c(l, f)}{c(l, f_0)} \right] r(f)df \quad (20)$$

or

$$n_{\text{tot}}(p, \alpha, l) = q(l)i(p, \alpha, l), \quad (21)$$

where  $i(p, \alpha, l)$  is defined as

$$i(p, \alpha, l) = \int_0^\infty w(p, f)(f/f_0)^2 \left[ \alpha + (1 - \alpha) \frac{c(l, f)}{c(l, f_0)} \right] r(l, f) df. \quad (22)$$

Equation (20) is used to define the terms  $I$  and  $Q$  appearing in the margin eq. (2) in the main body of the text, where the capital letters refer to dB quantities. In the field measurements,  $I$  has been determined by numerical integration for each measured line given the fitted values for  $p$  and  $\alpha$ , and given the measured frequency dependence of  $r(f)$  for the test repeater. The individual contributions of ACXT and FEXT to the power sum  $Q$  were then determined by:

$$q_{\text{ACXT}} = a_A = \alpha q(l) = \alpha \frac{n_{\text{tot}}}{i}, \quad (23)$$

where  $n_{\text{tot}}$  is the measured noise power sum. Also,

$$q_{\text{FEXT}} = a_F(l)c(l, f_0) = (1 - \alpha)q(l) = (1 - \alpha) \frac{n_{\text{tot}}}{i}. \quad (24)$$

The distributions of  $a_A$  and  $a_F(l)$  obtained by the use of eqs. (23) and (24) with the field measurement data are plotted in Figs. 14 and 15 and discussed in Section 4.4. In the plot of Fig. 15,  $l$  is approximately 6000 feet so that  $a_F(l)$  represents the equal-level FEXT coupling for a full-length repeater section.

## REFERENCES

1. K. E. Fultz and D. B. Penick, "The T1 Carrier System," B.S.T.J. 44, No. 7 (September 1965), pp. 1405-51.
2. H. Cravis and T. V. Crater, "Engineering of T1 Carrier System Repeated Lines," B.S.T.J. 42, No. 1 (March 1963), pp. 431-86.
3. G. F. Erbrecht et al., B.S.T.J., this issue.

